Biomimetic Synthesis and Characterization of Magnetic Proteins (Magnetoferritin)

Kim K. W. Wong,[†] Trevor Douglas,[†] Savas Gider,[‡] David D. Awschalom,[‡] and Stephen Mann*,[†]

School of Chemistry, University of Bath, Bath BA2 7AY, U.K., and Department of Physics, University of California, Santa Barbara, California 93106

Received June 12, 1997. Revised Manuscript Received September 30, 1997[⊗]

A new synthesis of the magnetic protein magnetoferritin is reported. Addition of increments of Fe(II) to anaerobic solutions of the demetalated protein, apoferritin, at pH = 8.6 and 65 °C, followed by stoichiometric amounts of the oxidant trimethylamine-*N*-oxide (Me_3NO), results in the formation of a dispersed magnetic bioinorganic nanocomposite. By limiting the Fe:protein ratio to not more than ~140 atoms/protein molecule and the Fe(II):Me_3NO ratio to 3:2 in each increment, ferrimagnetic nanocrystals of magnetite/maghemite (Fe_3O_4)/(γ-Fe_2O_3) are synthesized in the 8 nm diameter protein cage. Controlling the number of stepwise cycles of the Fe(II)/oxidant additions produces biomimetic proteins with different iron loadings (100, 260, 530, 1000, 2040, and 3150 Fe atoms/protein molecule) and concomitant changes in the size of the inorganic nanocores. Magnetoferritins prepared with less than 1000 Fe atoms/molecule were discrete nanocomposites with protein-encapsulated magnetic cores. Samples with higher iron loadings were aggregated on the TEM grid and showed a progressive increase in the number of cores with dimensions greater than the protein cavity. The temperature-dependent magnetic properties of magnetoferritins with different Fe loadings were studied by SQUID magnetometry. An approximately linear dependence of the superparamagnetic blocking temperature with iron loading was determined.

Introduction

The iron storage protein, ferritin, consists of a central core of hydrated iron (III) oxide encapsulated within a multisubunit protein shell.[1,2] The polypeptide shell is self-assembled prior to inorganic mineralization with the consequence that the nucleation and growth of the iron oxide are spatially confined within an 8 nm diameter protein cage. In natural mammalian ferritin, the core is composed of an antiferromagnetic iron oxide similar to the mineral ferrihydrite.[3,4] The presence of molecular channels within the protein shell makes it possible to remove the inorganic phase in vitro by reductive dissolution.[5,6] This procedure produces a demetalated protein, called apoferritin, which can be subsequently remineralized by chemical procedures.[7]

The reconstitution of ferrihydrite cores in ferritin has been used to study the functional properties of the apoferritin molecule with regard to the catalysis of Fe(II) oxidation and nucleation of ferrihydrite specifically within the protein compartment.[8−10] Recently, we have adopted a similar strategy for the controlled chemical synthesis of a range of biomimetic ferritin proteins. For example, manganese oxide,[11−13] uranium oxide,[11,14] and cadmium sulfide[15] nanoparticles have been prepared within the polypeptide cage of horse spleen apoferritin. In another study, an artificial magnetic protein, termed magnetoferritin, was synthesized by reconstitution of the inorganic cores with the ferrimagnetic mineral magnetite (Fe_3O_4).[16,17] The resulting material is a

* To whom correspondence should be addressed.
[†] University of Bath.
[‡] University of California.
[⊗] Abstract published in *Advance ACS Abstracts*, December 15, 1997.

(1) Harrison, P. M.; Artymuik, P. J.; Ford, G. C.; Lawson, D. M.; Smith, J. M. A.; Treffry, A.; White, J. L. In *Biomineralization: Chemical and Biochemical Perspectives*; Mann, S., Webb, J., Williams, R. J. P., Eds.; VCH Publishers: Weinheim, 1989; pp 257−294.
(2) Ford, G. C.; Harrison, P. M.; Rice, D. W.; Smith, J. M. A.; Treffry, A.; White, J. L.; Yariv, J. *Philos. Trans. R. Soc. London B* **1984**, *304*, 551.
(3) Mann, S., Bannister, J. V., Williams, R. J. P. *J. Mol. Biol.* **1986**, *188*, 225.
(4) St Pierre, T. G.; Bell, S. H.; Dickson, D. P. E.; Mann, S.; Webb, J.; Moore, G. R.; Williams, R. J. P. *Biochim. Biophys. Acta* **1986**, *870*, 127.
(5) Treffry, A.; Harrison, P. M. *Biochem. J.* **1978**, *171*, 313.
(6) Funk, F.; Lenders, J.-P.; Crichton, R. R.; Schneider, W. *Eur. J. Biochem.* **1985**, *152*, 167.
(7) Macara, I. G.; Hoy, G.; Harrison, P. M. *Biochem. J.* **1972**, *126*, 151.
(8) Lawson, D. M.; Treffry, A.; Artymiuk, P. J.; Harrison, P. M.; Yewdall, S. J.; Luzzago, A.; Cesareni, G.; Levi, S.; Arosio, P. *FEBS Lett.* **1989**, *254*, 207.
(9) Lawson, D. M.; Artymiuk, P. J.; Yewdall, S. J.; Smith, J. M. A.; Livingstone, J. C.; Treffry, A.; Luzzago, A.; Levi, S.; Arosio, P.; Cesareni, G.; Thomas, C. D.; Shaw, W. V.; Harrison, P. M. *Nature* **1991**, *349*, 541.
(10) Wade, V. J.; Levi, S.; Arosio, P.; Treffry, A.; Harrison, P. M.; Mann, S. *J. Mol. Biol.* **1991**, *221*, 1443.
(11) Meldrum, F. C.; Wade, V. J.; Nimmo, D. L.; Heywood, B. R.; Mann, S. *Nature* **1991**, *349*, 684.
(12) Mackle, P.; Charnock, J. M.; Garner, C. D.; Meldrum, F. C.; Mann, S. *J. Am. Chem. Soc.* **1993**, *115*, 8471.
(13) Meldrum, F. C.; Douglas, T.; Levi, S.; Arosio, P.; Mann, S. *J. Inorg. Biochem.* **1995**, *58*, 59.
(14) Hainfeld, J. F. *Proc. Natl. Acad. Sci. U.S.A.* **1992**, *89*, 11064.
(15) Wong, K. K. W.; Mann, S. *Adv. Mater.* **1996**, *8*, 928.
(16) Meldrum, F. C.; Heywood, B. R.; Mann, S. *Science* **1992**, *257*, 522.

S0897-4756(97)00421-3 CCC: $15.00
Published on Web 01/19/1998

dispersed bioinorganic ferrofluid and has been shown to have significant potential as a biocompatible, nanodimensional magnetic resonance contrast agent[18−20] and immunomagnetic label for cell separation.[21]

Studies with ferritin reconstituted with ferrihydrite cores have shown that different particle sizes can be synthesized by control over the Fe:protein ratio in the reaction mixture and that the corresponding changes in superparamagnetism can be followed by SQUID magnetometry.[22,23] In contrast, previous reports on magnetoferritin have focused on the synthesis, characterization, and properties of samples containing only high loadings of iron (approximately 3000 Fe atoms).[22−25] Because the magnetic properties of magnetoferritin should be dependent on the particle size of the associated inorganic cores, the ability to fine-tune the reconstitution process could have potential benefits in a range of applications.

In this paper, we report a new synthesis procedure for magnetoferritin. Our method has several important advantages over that reported previously.[16] By undertaking the synthesis under anaerobic conditions in the presence of stoichiometric amounts of oxidant, we minimize the formation of nonmagnetic ferric oxides such as ferrihydrite. Furthermore, we employ a series of cycles of incremental addition of Fe(II) followed by oxidant, to augment the specific nucleation of the magnetic phase within the protein cavity and thereby reduce any adventitious precipitation in bulk solution. This procedure also enables us to terminate the reconstitution process at any given time so that samples with different core loadings can be routinely prepared. High-resolution electron microscopy, electron diffraction and SQUID magnetometry have been used to characterize the bioinorganic nanocolloids synthesized.

Experimental Section

Preparation of Apoferritin. Apoferritin was prepared by demineralization of horse spleen ferritin according to established procedures.[5,6] Cadmium-free horse spleen ferritin (250 mg; 5 mL; Boehringer Mannheim) was placed into a dialysis bag (molecular weight cutoff 12 000−14 000) and diluted (×5) with sodium acetate buffer (0.1 M; 25 mL, pH 4.5). The bag was floated in ∼800 mL of buffer and purged with N_2 for 15−30 min, when thioglycolic acid (TGA; 2.0 mL; ∼2 g; ∼0.02 M) was added while continuously purging with N_2. After ∼2 h a further 1 mL of TGA was added and dialysis continued for another 1 h. The buffer was refreshed, purged with N_2 for 15−30 min, and the demineralization procedure repeated. On completion of the second treatment the ferritin solution was usually colorless; if not, the above procedure was repeated with fresh buffer. The N_2 purge was stopped and the apoferritin solution dialyzed against saline (0.15 M; 2 L) for 1 h with stirring. The saline was refreshed (3 L) and the product dialyzed, with stirring, overnight in a cold room. Apoferritin solutions stored for long periods contained 0.001% w/w NaN_3. Apoferritin concentrations were determined by the method of Lowry.[26] Yields of apo-ferritin ranged from 65 to 80%.

Synthesis of Magnetoferritin. Trimethylamine-*N*-oxide (Me_3NO) was heated in an oven at 80 °C for ∼15−30 min to remove Me_3N. Aqueous solutions of Me_3NO (114 mg/15 mL, 0.07 M) and ferrous ammonium sulfate (Fe^{2+}; 600 mg/15 mL, 0.1 M) were prepared and gently deaerated with Ar for ∼30 min before use. 3-[(1,1-Dimethyl-2-hydroxyethyl)amino]-2-hydroxy-propanesulfonic acid (AMPSO) buffer solution (50 mM; 500 mL; buffered to pH 8.6 with 2.0 M NaOH) was stirred and deaerated with Ar for not less than 1 h. Apoferritin (100 mg; 0.22 μmol) was added to give a protein concentration of 0.44 M. Gentle stirring and deaeration with Ar were continued for a further 30 min, after which the reaction vessel was placed in a preheated (65 °C) oil bath and the contents were allowed to reach equilibrium. Purging with Ar through the buffered protein solution was ceased, but the reaction vessel was kept under a positive pressure of Ar.

Aliquots of Fe(II) (typically, up to 300 μL; 30.60 μmol; 140 Fe atoms/apoferritin molecule) and Me_3NO (typically, up to 300 μL; 20.50 μmol) were added dropwise to the reaction solution using gastight glass barrelled syringes. In general, each addition of Fe(II) was followed by a stoichiometric aliquot of Me_3NO (3Fe(II):2Me_3NO) and the solution left for 15 min before repeating the stepwise procedure. The first and second increments of Fe(II) solution contained ≈50 Fe atoms/protein molecule, whereas later additions were increased to ≈138 Fe atoms/molecule. No addition of Me_3NO was made following the first addition of Fe(II) in order to scavenge residual oxygen in the system. Samples (∼5−10 mg) with theoretical loadings of 100, 260, 530, 1000, 2040, and 3150 Fe atoms/protein molecule were removed sequentially from the reaction solution and dialyzed at 4 °C against distilled water (pH = 6.0). In a typical experiment, 10 stepwise cycles were undertaken to give a loading of 1000 Fe atoms/molecule and was achieved within 2.5 h at pH 8.6 and 65 °C.

Morphological and Structural Analysis. The morphology, particle size distributions, and structure of the iron oxide cores of magnetoferritins prepared with different metal loadings were determined by transmission electron microscopy (TEM). Magnetoferritin samples were deposited onto carbon-coated, Formvar-covered copper grids by air-drying of dilute solutions. In addition, some samples were negatively stained with 1% uranyl acetate solution. A JEOL 1200EX analytical transmission electron microscope operating at 60−120 kV was used. Electron diffraction patterns (camera length = 0.8 m) and lattice imaging were recorded on a JEOL 2000FX TEM operating at 200 keV. Particle size histograms were obtained by measuring individual iron oxide cores from enlarged micrographs. Approximately 150 discrete particles, as well as approximately 50 individual cores located within aggregated clusters on the TEM grid, were measured for each sample.

SQUID Magnetometry. Studies of the static magnetic properties of magnetoferritins with different Fe loadings (different particle sizes) were made with an rf SQUID magnetometer. Magnetization measurements were done in a commercial rf SQUID magnetometer[27] at temperatures ranging from 2 to 200 K and fields up to 5 T. The rf SQUID is capable of resolving changes as small as 10^{-7} emu for dc magnetization measurements with a time scale of approximately 8 s (the time for the sample to be scanned through the second-order gradiometer coils). Each magnetoferritin sample consisted of 0.1−0.5 mg of protein and a variable mass of mineral in the core. The measured magnetizations were

(17) Douglas, T.; Bulte, J. W. M.; Dickson, D. P. E.; Frankel, R. B.; Pankhurst, Q. A.; Moskowitz, B. M.; Mann, S. *ACS Symp. Ser.* **1995**, *585*, 19.
(18) Bulte, J. W. M.; Douglas, T.; Mann, S.; Frankel, R. B.; Moskovitz, B. M.; Brooks, R. A.; Baumgarner, C. D.; Vymazel, J.; Strub, M.-P.; Frank, J. A. *J. Magn. Reson. Imaging* **1994**, *4*, 497.
(19) Bulte, J. W. M.; Douglas, T.; Mann, S.; Frankel, R. B.; Moskovitz, B. M.; Brooks, R. A.; Baumgarner, C. D.; Vymazel, J.; Strub, M.-P.; Frank, J. A. *Invest. Radiol.* **1994**, *29*, S214.
(20) Bulte, J. W. M.; Douglas, T.; Mann, S.; Vymazal, J.; Laughlin, B. S.; Frank, J. A. *Acad. Radiol.* **1995**, *2*, 871.
(21) Zborowski, M.; Bor Fur, C.; Green, R.; Baldwin, N. J.; Reddy, S.; Douglas, T.; Mann, S.; Chalmers, J. J. *Cytometry* **1996**, *24*, 251.
(22) Gider, S.; Awschalom, D. D.; Douglas, T.; Mann, S.; Chaparala, M. *Science* **1995**, *268*, 77.
(23) Gider, S.; Awschalom, D. D.; Douglas, T.; Wong, K. K. W.; Mann, S.; Cain, G. *J. Appl. Phys.* **1996**, *79*, 5324.
(24) Pankhurst, Q. A.; Betteridge, S.; Dickson, D. P. E.; Douglas, T.; Mann, S.; Frankel, R. B. *Hyperfine Interact.* **1994**, *91*, 847.
(25) Moskowitz, B. M.; Frankel, R. B.; Walton, S. A.; Dickson, D. P. E.; Wong, K. K. W.; Douglas, T.; Mann S. *J. Geophys. Res.* **1997**, *102*, 22671.
(26) Peterson, G. L. *Anal. Biochem.* **1977**, *83*, 346.
(27) MPMS-5S, Quantum Design, San Diego, CA 92121.

normalized with respect to the protein mass of horse spleen ferritin (70 wt %) in order to compare the samples. The samples were prepared by drying in air on a 25 × 25 mm polypropylene film at 40 °C. Polypropylene was used because it was found to have only a small diamagnetic moment (8.3×10^{-8} emu/g per 25 × 25 mm sample substrate) which was temperature independent. The samples were mounted on a twisted copper wire pair (0.5 mm diameter, 99.9% pure) in order not to introduce any additional diamagnetic background. The moment of the polypropylene film was subtracted from the magnetic measurements.

Results and Discussion

Synthesis and Structure of Magnetoferritin. Addition of a theoretical loading of 100 Fe atoms/protein molecule resulted in a light brown coloration of the reaction mixture. Increasing the metal-ion loading by stepwise addition of Fe(II) and Me_3NO solutions resulted in a darkening of the reaction solution without bulk precipitation. Not more than 200 atoms of Fe/protein molecule can be added per addition because higher levels exceeded the solubility product of $Fe(OH)_2$, resulting in a finely dispersed, bulk white precipate that turned brown and sedimented on exposure to air. Although most of the protein remained in solution throughout, a small amount of a dark brown magnetic precipitate was observed toward the end of the reaction (6 h). Dispersed samples were extracted from the reaction mixture and stored as 3 mg/mL solutions in distilled water at 4 °C. In general, these were significantly more stable with respect to sedimentation than analogous samples stored in NaCl solutions. For example, magnetoferritins containing more than 2000 Fe atoms/molecule remained in solution for 4 weeks when stored in distilled water but flocculated within 24 h in the presence of 0.15 M NaCl. This suggests that protein aggregation is facilitated by electrostatic shielding of the charged ferritin molecules. Moreover, horse spleen ferritin is generally stable under these electrolyte conditions, suggesting that the relatively long exposure to high temperature and pH of the highly loaded magnetoferritins modifies the surface charge of the protein shell.

In general, samples prepared with different mineral loadings showed well-defined rounded or irregular nanoparticles when imaged by TEM (Figure 1). In contrast, the reaction product produced under identical chemical conditions but in the absence of apoferritin gave a bulk precipitate consisting of irregular micron size particles (data not shown). Lattice images of individual magnetoferritin cores showed that many of the intra-protein particles were single domain crystals (Figure 2). The spacings and angles between lattice fringes were consistent with a cubic ($Fd3m$) spinel phase of magnetite (Fe_3O_4) or maghemite (γ-Fe_2O_3). Selected area electron diffraction analysis of the iron oxide cores also showed characteristic d spacings (experimental values in nm; 0.490 {111}, 0.299 {220}, 0.255 {311}, 0.211 {400}, 0.175 {422}, 0.165 {511}, 0.151 {440}) for a magnetite or maghemite lattice. The additional weak superlattice reflections that distinguish maghemite from magnetite were not observed.

The synthesis reported here is significantly different from that described previously for magnetoferritin, which employed a more empirical approach involving aerial oxidation.[16] The use of Me_3NO as a one-electron oxidant, under controlled chemical conditions, permits much greater fine-tuning and reproducibility in the synthesis of the magnetite/maghemite cores. The reaction stoichiometry was empirically fixed at a mole ratio of [Fe(II)]:[Me_3NO] = 3:2 for each stepwise addition of the two reagents, that is, assuming the reaction

$$3Fe(II) + 2Me_3NO + 4H_2O \rightarrow Fe_3O_4 + 2Me_3N + 6H^+ + H_2O_2$$

Previous results on the reconstitution of apoferritin with the iron(III) oxide ferrihydrite (FeOOH) indicate that the kinetics for Fe(II) oxidation are dependent on the protein to metal ion ratio.[28] A protein-directed pathway, involving a two-electron-transfer process to dioxygen molecules located at the ferroxidase centers in the H-chain subunit (ca. 15% of the horse spleen heteropolymer), was observed when small increments (24 Fe(II)/molecule) of iron were added. In contrast, increments >50 Fe(II)/molecule resulted in a four-electron exchange on the surface of the mineral core. As all the increments in our experiments contained >50 Fe atoms/molecule, it is unlikely that the ferroxidase centers play a significant role in the formation of the magnetite/maghemite cores.

Characterization of Magnetoferritins with Different Core Loadings. Magnetoferritin prepared with a theoretical loading of 100 Fe atoms/molecule consisted of low-contrast discrete nanoparticles that were difficult to image in the electron microscope. Measurements of the particle sizes of those cores that could be clearly defined gave a mean value of 4.0 nm with a distribution in the range 2−6 nm (Figure 3a, Table 1). All the measured cores were therefore smaller than the 8.5 nm diameter of the polypeptide cavity, indicating that nucleation and growth of the spinel phase was specifically confined within the protein. Increasing the loading to 260 Fe atoms/molecule resulted in discrete electron-dense spherical nanoparticles of mean diameter, 5.7 nm (Figure 1a). A few particles (<10%) appeared slightly elongated. The particle size measurements (Figure 3b, Table 1) gave a narrow distribution of cores with the range 3−9 nm. Negative staining of the sample clearly showed that the mineral cores were encapsulated within the polypeptide shell (Figure 1b). Similar observations were made for a magnetoferritin sample prepared with a theoretical loading of 530 Fe atoms/molecule (Figure 1c), except that the discrete spherical cores were slightly larger (Table 1). As before, the spatial constraint imposed by the polypeptide shell was clearly reflected in the particle size distribution (Figure 3c) which showed an abrupt decrease in the frequency of particles from 50% of the population in the 6.6−7.5 nm group to less than 5% with dimensions 7.5−9 nm. A small percentage of magnetoferritin particles (<5%) appeared to be aggregated on the electron microscope grid.

Significant differences were observed for magnetoferritin prepared with a theoretical loading of 1000 Fe atoms/molecule. Although the sample remained dispersed in the bulk phase and discrete cores were observed by electron microscopy, approximately 70% of

(28) Sun, S.; Chasteen, N. D. *J. Biol. Chem.* **1992**, *267*, 25160.

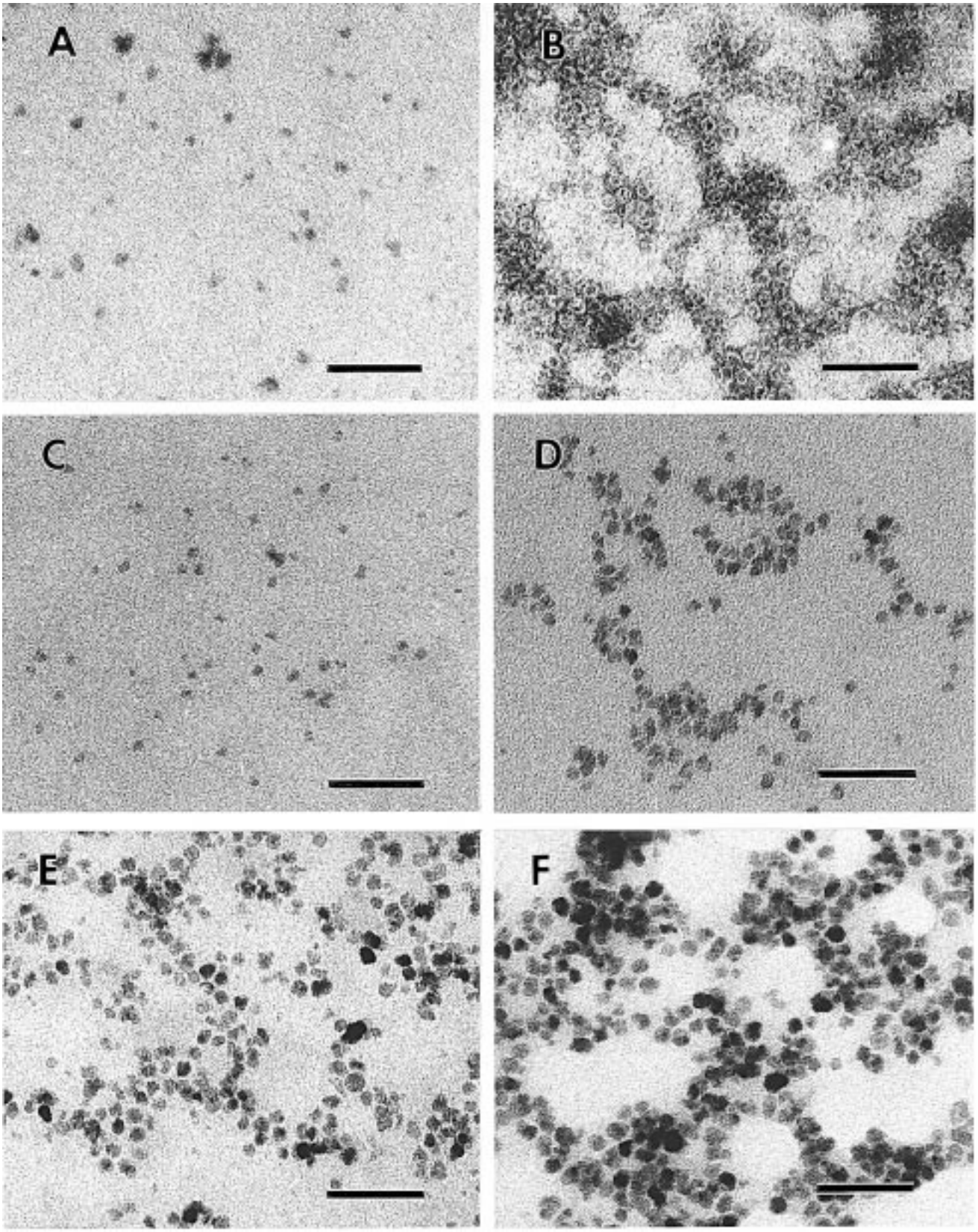

Figure 1. TEM micrographs of magnetoferritins. (a) 260 Fe atoms/molecule, unstained, showing discrete electron-dense inorganic cores. (b) 260 Fe atoms/molecule, stained with uranyl acetate, showing encapsulation of inorganic cores by intact protein shell (white halo around each particle). (c) 530 Fe atoms/molecule, unstained. (d) 1000 Fe atoms/molecule, unstained. (e) 2040 Fe atoms/molecule, unstained. (f) 3150 Fe atoms/molecule, unstained. Scale bars in all figures = 50 nm.

the individual nanoparticles were aggregated on the TEM grid (Figure 1d). These observations suggest that reaction times of over 2 h produce modifications in the surface charge of the protein that result in increased aggregation during air-drying. The discrete cores were spherical and had a mean diameter of 7.5 nm, whereas individual nanoparticles present within the aggregated material were significantly larger on average (mean =

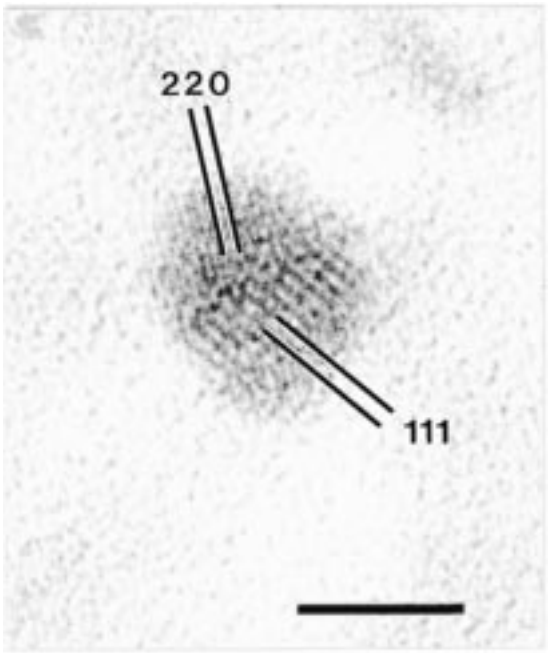

Figure 2. High-resolution TEM micrograph of a single magnetoferritin core. The lattice spacings (0.485 nm {111}, 0.299 {220}) and angles (111 Λ 220 = 35°) between fringes correspond to a view down the [110] zone of the mineral magnetite/maghemite (space group $Fd3m$). Scale bar = 5 nm.

9.4 nm, Table 1). Particle size distributions (Figure 4a) indicated that almost half of the aggregated particles exceeded the dimensions of the protein cavity, compared with approximately 10% of the discrete cores (Table 1).

Similar observations were made for magnetoferritins prepared with theoretical loadings of 2040 or 3150 Fe atoms/molecule. Over 90% and 95% of these cores, respectively, were aggregated on the TEM grid, although the cores were not intergrown or contiguous (Figure 1e,f). Whereas the majority of cores prepared with 2040 Fe atoms/molecule had a rounded shape, those in the sample containing 3150 Fe atoms/molecule were predominantly regular in morphology, often with faceted edges. The corresponding particle size measurements showed a continuing increase in mean size and number of particles larger than 9.5 nm (Table 1, Figure 4b,c).

The data suggest that prolonged reaction times (>2 h at pH 8.6, 65 °C) result in increasing numbers of magnetoferritin cores with dimensions greater than the protein cavity. This is particularly the case for cores present in aggregated material suggesting that the organic shell could be partially disrupted by thermal or chemical degradation, so that some crystals are no longer confined within the supramolecular cage. However, polyacrylamide gel electrophoresis of disassembled magnetoferritin showed no significant changes in the molecular weight of the subunits compared with the native protein.[18] Another possibility is that continued growth of the mineral cores over extended reaction times gives rise to nanoparticles that traverse the protein shell by crystal growth through the molecular channels present within the polypeptide coat.

As the theoretical iron loading is increased, the general trend is for increasingly larger cores (Table 1). However, the measured core diameters are consistently

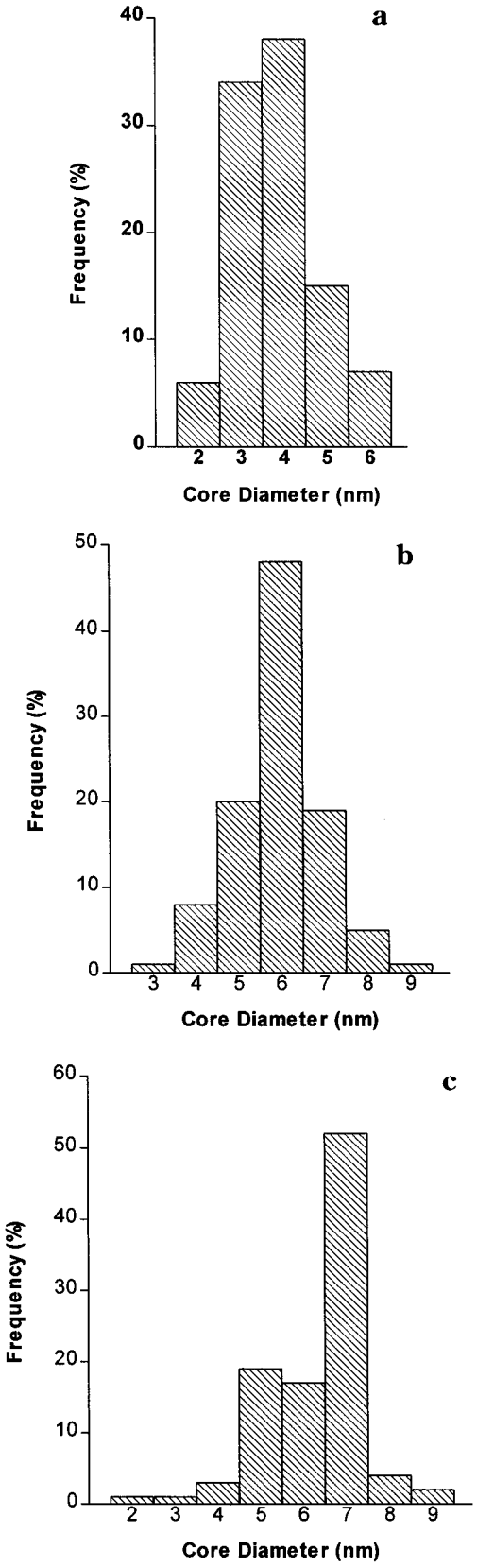

Figure 3. Particle size histograms of discrete electron-dense cores for magnetoferritns prepared with loadings of (a) 100, (b) 260, and (c) 530 Fe atoms/molecule.

larger than the theoretical core diameters calculated for a spherical particle of uniform density (Table 1). Similar discrepancies have been observed for other biomimetic ferritins in which the protein has minimal cata-

Table 1. Comparison of Calculated Theoretical versus Measured Iron Core Diameters

theoretical iron loading; atoms/protein molecule	mean iron core diameters (discrete/aggregated); /nm	std dev/nm	% of cores >9.5 nm (discrete/aggregated)	calcd theor iron core diameters/nm
100	4.0	1.0	0	1.7
260	5.7	1.0	0	2.3
530	6.4	1.2	0	2.9
1000	7.5/9.4	1.3/1.6	10/55	3.6
2040	7.4/10.6	1.4/1.9	25/70	4.6
3150	8.4/10.4	1.5/1.8	30/80	5.2

lytic activity, and growth is determined by size-dependent autocatalysis at the mineral surface.[11,13] Thus, addition of further increments of Fe(II) and Me_3NO to preformed magnetite/maghemite cores appears to enhance the crystal growth of a population of larger nanoparticles at the expense of protein molecules containing smaller crystallites. In fact, polyacrylamide gel electrophoresis indicated that apoferritin molecules were still present even after loadings of 2000 Fe atoms/protein molecule in the magnetoferritin synthesis.[18,29] The presence of a population of nonreconstituted protein molecules explains why the theoretical core dimensions were always less than those measured experimentally.

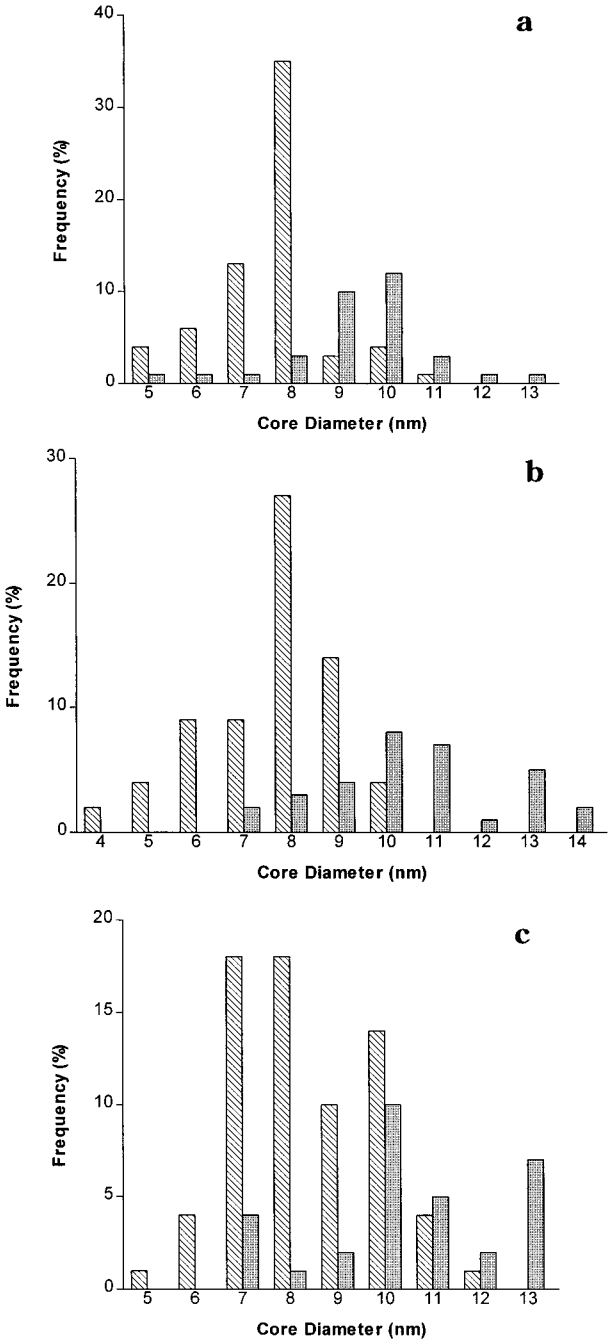

Figure 4. Particle size histograms of discrete (hatched) and aggregated (filled) cores for magnetoferritns prepared with loadings of (a) 1000, (b) 2040, and (c) 3150 Fe atoms/molecule.

Magnetic Properties of Magnetoferritins. The size dependence of the magnetic properties of the ferrimagnetic magnetoferritin were consistent with initial measurements of the fully loaded particles reported elsewhere.[18,22,23] No anomaly was observed in the remanence up to 150 K, and therefore evidence of the characteristic Verwey transition for magnetite was not obtained. This observation, together with Mössbauer data,[24] suggests that the mineral cores of magnetoferritin are predominantly maghemite (γ-Fe_2O_3) instead of magnetite (Fe_3O_4). Maghemite readily forms by aerial oxidation of magnetite, and this reaction would be facilitated by the high surface area of the magnetoferritin cores. In addition, although the stoichiometry of the redox reaction was experimentally set for magnetite deposition, decomposition of byproducts such as H_2O_2 would slowly release O_2 into the medium and induce further oxidation of Fe(II).[28]

Each magnetoferritin sample was superparamagnetic at temperatures above 100 K. At lower temperatures, the difference between the field-cooled and zero-field-cooled magnetization verses temperature curves was indicative of anisotropy in the maghemite cores as reported previously for a fully loaded magnetoferritin sample.[22] Like the natural ferritin, the magnetoferritin also displayed an increase in the superparamagnetic blocking temperature with increasing volume from almost 10 to 100 K for iron loading from 250 to 3100 ions, respectively (Figure 5). The data point for the sample loaded with 2040 Fe atoms/protein molecule appeared spurious, possibly because of inaccuracies in estimating the average core volume from aggregated samples on the TEM grid. Alternatively, the lower blocking temperature of this sample compared with that for the similar putative volume for a loading of 3150 Fe/protein, might arise from the increased regularity of the nanoparticles formed at the higher loading, which results in a larger anisotropy constant and increased energy barrier for thermal activation of the magnetic dipole. Except for the data point at 2040 Fe/molecule, the blocking temperature dependence appears to be linear within 95% confidence limits. Moreover, the plot extrapolates to zero, similar to that observed for native ferritin.[22]

(29) Wong, K. K. W.; Mann, S., unpublished observations.

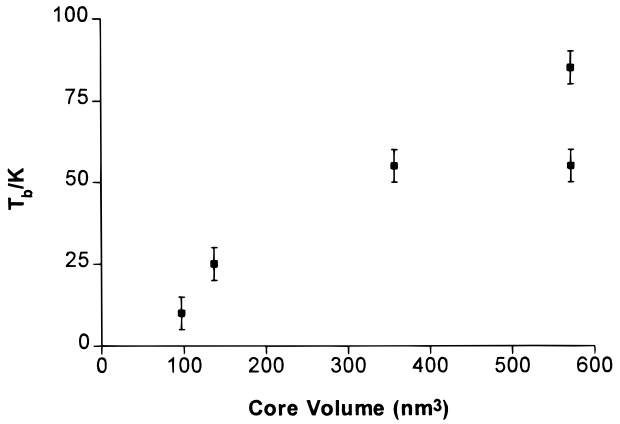

Figure 5. Plot of particle volume against superparamagnetic blocking temperature (T_b) for synthesized magnetoferritins. The lower and higher T_b values plotted against a volume of approximately 600 nm^3 correspond to loadings of 2040 and 3150 Fe atoms/protein molecule, respectively.

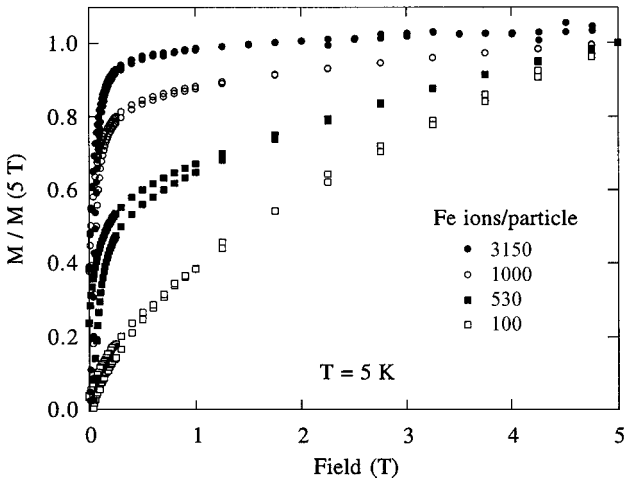

Figure 6. Plot of normalized magnetization (M/M(5 T)) against applied field (T) for magnetoferritins with different Fe/molecule loadings. The data were recorded at a temperature of 5 K.

The larger moment of the magnetoferritin cores, as compared to the antiferromagnetic cores of natural ferritin, allowed for a more complete study of hysteresis in samples with different core sizes. In particular, the field required to saturate the moment was found to increase as the particle volume decreases (Figure 6). This is consistent with a decrease in the moment per particle for superparamagnetic particles whose magnetization is well described by a Langevin function. In addition, the coercive field was observed to increase as the volume decreased (Figure 7a), suggesting that the likelihood of forming magnetic domains becomes less favorable as the volume decreases. Alternatively, if the anisotropy constant K does not change, the decrease in the moment M implies an increase in the coercive field $H_c = 2K/M$ for coherent reversal of magnetization within the Stoner−Wohlfarth model of single domain noninteracting particles. Finally, the remanence was found to decrease by 3 orders of magnitude while the volume changes by less than 1 order of magnitude (Figure 7b). Thus the magnetic stability of the magnetoferritin cores was extremely sensitive to particle size.

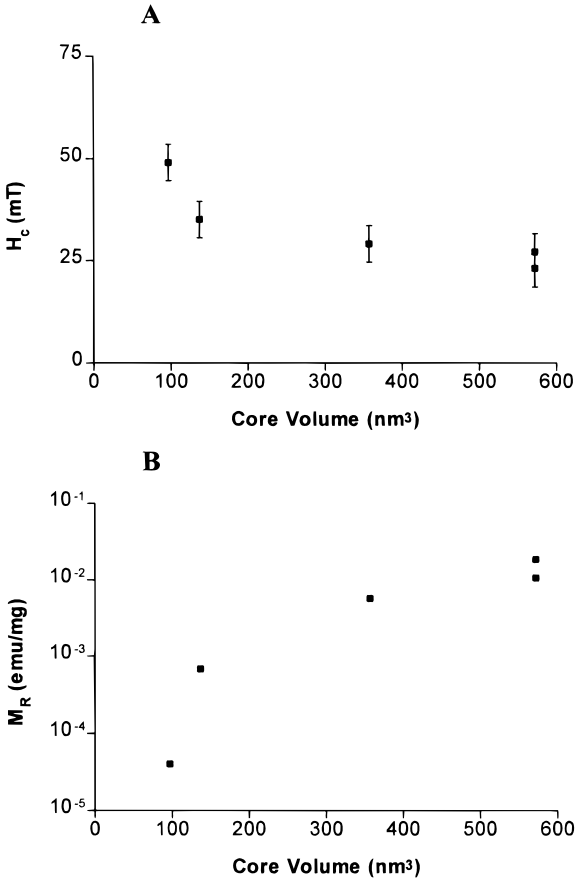

Figure 7. (a) Plot of coercive field (H_c) against particle volume and (b) magnetic remanance (M_R) against particle volume for synthesized magnetoferritins. The two (similar) values at a volume of approximately 600 nm^3 correspond to loadings of 2040 and 3150 Fe atoms/protein molecule.

Conclusions

The results presented in this paper indicate that magnetoferritin can be synthesized by a stepwise procedure involving incremental addition of stoichiometric amounts of Fe(II) and Me_3NO to protein solutions maintained under N_2 at pH = 8.6 and 65 °C. Magnetic proteins containing inorganic nanoparticles of different size can be synthesized, although the core volumes are larger than those predicted on the basis of a homogeneous distribution of Fe atoms among the protein molecules. Samples with theoretical loadings greater than 1000 Fe atoms/molecule had a tendency to aggregate on the TEM grid and contained significant numbers of magnetite/maghemite cores greater in size than the diameter of the protein cavity. These observations, taken in conjunction with associated magnetic measurements, indicate that the optimal conditions for preparing magnetoferritins involve theoretical loadings of approximately 1000 Fe atoms/molecule. Magnetic proteins synthesized under these conditions should be useful in a range of biomedical applications.

Acknowledgment. We thank the BBSRC, UK for financial support of a postdoctoral fellowship to K.K.W.W. and the US Air Force Office of Scientific Research (Grant F49620-96-1-0018).

CM970421O